Revisiting anomalous $B(E2; 4_1^+ \rightarrow 2_1^+)/B(E2; 2_1^+ \rightarrow 0_1^+)$ values in ^{98}Ru and ^{180}Pt

E. Williams,[1] C. Plettner,[1] E. A. McCutchan,[1] H. Levine,[1] N. V. Zamfir,[1,2] R. B. Cakirli,[1,3] R. F. Casten,[1] H. Ai,[1] C. W. Beausang,[1,4] G. Gürdal,[1,5] A. Heinz,[1] J. Qian,[1] D. A. Meyer,[1] N. Pietralla,[6,7] and V. Werner[1]

[1]*A.W. Wright Nuclear Structure Laboratory, Yale University, New Haven, Connecticut 06511, USA*

[2]*National Institute for Physics and Nuclear Engineering, Bucharest-Maturele, Romania*

[3]*Istanbul University, Department of Physics, Turkey*

[4]*Department of Physics, Richmond University, Richmond, Virginia 23173, USA*

[5]*Clark University, Worcester, Massachusetts 01610, USA*

[6]*State University of New York at Stony Brook, Stony Brook, New York 11794, USA*

[7]*Institut für Kernphysik, Universität zu Köln, D-50937 Köln, Germany*

(Received 8 May 2006; published 11 August 2006)

Recently, a set of nine nonmagic nuclei with anomalous values of the $B(E2)$ ratio $B_{4/2} \equiv B(E2; 4_1^+ \rightarrow 2_1^+)/B(E2; 2_1^+ \rightarrow 0_1^+) < 1$ were identified. Such values are outside the range allowed by current collective models. In the present work, the $B(E2; 4_1^+ \rightarrow 2_1^+)$ values for two of these nuclei, ^{98}Ru and ^{180}Pt, were re-measured to determine if the current literature values for these nuclei are correct. ^{98}Ru was studied in a ^{27}Al(^{98}Ru,^{98}Ru*) Coulomb excitation experiment in inverse kinematics, while the lifetime of the 4_1^+ state in ^{180}Pt was measured in a ^{122}Sn(^{62}Ni, $4n$)^{180}Pt recoil distance method (RDM) experiment. For both nuclei, the remeasured $B_{4/2}$ values are well above 1, removing the deviations from collective models.

DOI: 10.1103/PhysRevC.74.024302 PACS number(s): 21.10.Ky, 21.60.Ev, 27.60.+j, 27.70.+q

I. INTRODUCTION

Surveys of the nuclear chart have revealed several signatures of collective behavior that we now almost casually use as simple means of identifying structure. Deviations from this expected behavior have come to serve as subtle hints that our understanding of the collective behavior of nuclei is somehow incomplete, and must be explored more closely. Quadrupole transition strengths in particular often play this role; the ratio $B_{4/2} \equiv B(E2; 4_1^+ \rightarrow 2_1^+)/B(E2; 2_1^+ \rightarrow 0_1^+)$ is a good example, as its value is 2 for a pure geometric vibrator [1] and 1.43 in the rotor model [2]. Most notably, $B_{4/2}$ is greater than 1 in all collective models, which generally reproduce the low-lying energy levels and transitions for nuclei with $R_{4/2} \equiv E(4_1^+)/E(2_1^+) > 2$.

In fact, the only cases in which $B_{4/2}$ is close to unity are those in which seniority is a good quantum number [3]—in other words, for nuclei near magic numbers, where $R_{4/2} < 2$ is typically observed. In a recent survey of all even-even nuclei for $40 \leqslant Z \leqslant 80$ [4], however, nine nonmagic nuclei were found to have $B_{4/2} < 1$. In all of these nuclei, the $B(E2; 2_1^+ \rightarrow 0_1^+)$ values are greater than 15 W.u., indicating collective behavior, in contrast to that suggested by their $B_{4/2}$ values, which are divergent from the predictions of collective models. While these discrepancies may simply point to experimental error, it is important to re-measure these anomalous ratios to investigate whether our current understanding of collectivity is in need of revision.

Thus, experiments on two of these anomalous nuclei, ^{98}Ru and ^{180}Pt, were conducted at the Wright Nuclear Structure Laboratory at Yale University. For ^{98}Ru, two different $B(E2; 4_1^+ \rightarrow 2_1^+)$ values exist in the literature [5,6]. The earlier measurement, a Coulomb excitation experiment, yielded a $B_{4/2}$ value of 1.41(27) [5], while the more recent measurement, using the recoil distance method, yielded a $B_{4/2}$ value of 0.38(11) [6]. ^{98}Ru was chosen because the $B_{4/2}$ value from the more recent measurement was the most extreme example of this deviation from collective models. ^{180}Pt, with $B_{4/2} = 0.9(2)$ [7], was selected because its listed $B_{4/2}$ value is far lower than those of the neighboring platinum nuclei, which exhibit almost constant $B_{4/2}$ ratios with changing neutron number, as shown in Fig. 1.

II. EXPERIMENTAL METHODS AND DATA ANALYSIS

In order to shed some light on these contradictory $B_{4/2}$ values and explore the extent to which these anomalous nuclei exhibit deviations from our current understanding of nuclear structure, we conducted two experiments: a ^{27}Al(^{98}Ru,^{98}Ru*) Coulomb excitation experiment in inverse kinematics, and a ^{122}Sn(^{62}Ni, $4n$)^{180}Pt lifetime measurement utilizing the recoil distance method (RDM). The details of each experiment are described below.

A. ^{98}Ru

For the ^{98}Ru experiment, a 289 MeV ^{98}Ru beam from the ESTU Tandem Accelerator of Yale University impinged upon a 0.54 g/cm^2-thick ^{27}Al target. The average beam intensity was 0.04 pnA. As shown in Fig. 2, known $B(E2)$ values for only a few low-lying transitions in ^{98}Ru have been established [5,6]; therefore, we wanted the multistep Coulomb excitation to be significantly weaker for levels above the 4_1^+ state in order to safely measure the $B(E2; 4_1^+ \rightarrow 2_1^+)$ value relative to these other known transitions. Thus, the beam energy was chosen to be 84.5% of the Coulomb barrier, and evidence of higher energy excitations was monitored throughout the experiment. Gamma rays emitted upon deexcitation were observed with the YRAST Ball array [8], which, in the configuration

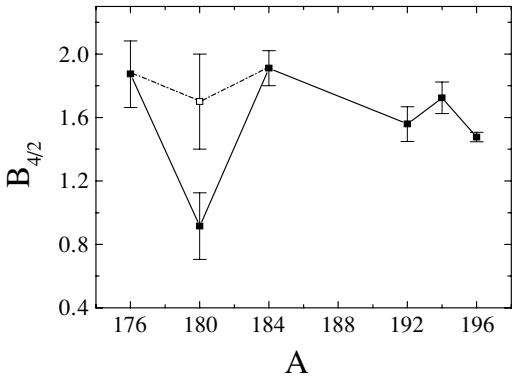

FIG. 1. Experimentally measured $B_{4/2}$ values for Pt isotopes. The solid data points label the previously reported measurements, in which an anomalously low $B_{4/2}$ value for ^{180}Pt was observed. The open data point marks the newly measured $B_{4/2}$ value for ^{180}Pt, in which the evolution of the $B_{4/2}$ value with respect to changing neutron number more closely matches the systematic behavior of the neighboring Pt isotopes.

for this experiment, consisted of seven Compton-suppressed EURISYS clover Ge-detectors oriented at 90° to the beam axis. A ^{152}Eu source was used for energy and efficiency calibrations. The master trigger was generated whenever a γ-ray of multiplicity one was detected. A total of 21 h of in-beam data were taken, corresponding to 2×10^7 events in the total projection. Room background was observed off-beam for 55 h.

Figure 3 shows a γ spectrum recorded by all clover detectors in coincidence with the 652 keV $2_1^+ \rightarrow 0_1^+$ transition. The prominent peaks seen in this figure, with the exception of the 652 keV random coincidences, correspond to the 668 keV $0_2^+ \rightarrow 2_1^+$, 745 keV $4_1^+ \rightarrow 2_1^+$, and 762 keV $2_2^+ \rightarrow 2_1^+$ transitions. The $B(E2; 4_1^+ \rightarrow 2_1^+)$ value was extracted by comparing the yields of the 762 keV $2_2^+ \rightarrow 2_1^+$ and 745 keV $4_1^+ \rightarrow 2_1^+$ transitions, as background contamination

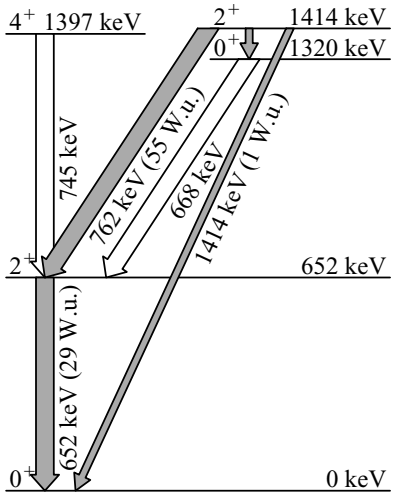

FIG. 2. Low-lying levels, transition energies, and transition strengths for ^{98}Ru. The open arrows mark the transition strengths extracted in this experiment.

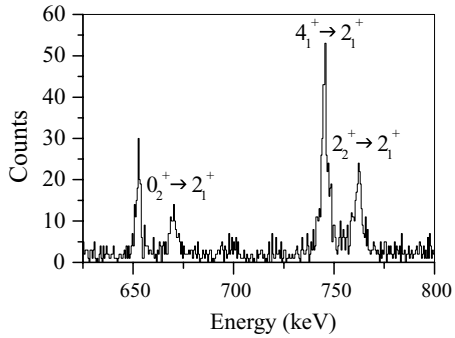

FIG. 3. Gate on 652 keV $2_1^+ \rightarrow 0_1^+$ transition in ^{98}Ru. With the exception of the random coincidence peak at 652 keV, the prominent peaks in the spectrum from left to right correspond to the 668 keV $0_2^+ \rightarrow 2_1^+$, 745 keV $4_1^+ \rightarrow 2_1^+$, and 762 keV $2_2^+ \rightarrow 2_1^+$ transitions.

in the singles spectrum made a relative measurement to the $B(E2; 2_1^+ \rightarrow 0_1^+)$ impossible. In addition, a $B(E2; 0_2^+ \rightarrow 2_1^+)$ value was extracted, by comparing the 762 keV $2_2^+ \rightarrow 2_1^+$ and the 668 keV $0_2^+ \rightarrow 2_1^+$ intensities.

To determine the $B(E2; 4_1^+ \rightarrow 2_1^+)$ and the $B(E2; 0_2^+ \rightarrow 2_1^+)$ values from this spectrum, we used the known $B(E2; 2_2^+ \rightarrow 2_1^+) = 55 \pm 10$ W.u. from the earlier Coulomb excitation experiment [5]. In extracting the $B(E2; 4_1^+ \rightarrow 2_1^+)$ and $B(E2; 0_2^+ \rightarrow 2_1^+)$, corrections were made for: (i) internal conversion, (ii) branching ratios, (iii) angular correlations of the de-excitation gamma rays, and (iv) background contamination.

In the singles spectrum, contaminant peaks almost degenerate with the 745 keV $4_1^+ \rightarrow 2_1^+$ and 762 keV $2_2^+ \rightarrow 2_1^+$ transitions were visible, and contributed random counts to the 652 keV coincidence spectrum. The 745 keV contaminant was due to activation in the target chamber, and was traced to a ^{52}Cr(p, α) reaction, produced by beta decay from ^{52}Mn. The 760 keV contaminant was too weak to be identified. Using the known lifetime of ^{52}Mn and background spectra taken both before and after the experiment, it was possible to subtract the number of counts in the 745 keV peak due to this contaminant. The overall correction to the 745 keV peak area in the coincidence spectrum was only 5%. For the 762 keV $2_2^+ \rightarrow 2_1^+$ transition, we were, in fact, able to resolve the 760 keV contaminant and the 762 keV peak in the coincidence spectrum sufficiently well for an estimate of the correction for this contaminant, approximately 20%, to be made.

The Winther-de Boer code [10] with a thick target integration was used to calculate total cross sections (σ) for the 2_1^+, 4_1^+, 0_2^+, and 2_2^+ states. Stopping power calculations were done for ^{98}Ru on ^{27}Al using SRIM [11]. The transitions and corresponding $B(E2)$ values used in the calculations can be found in Fig. 2, and in Table I. While test calculations included transitions that were unobserved in our experiment, as well as the quadrupole moment of the 2_1^+ state, we determined that their inclusion had a negligible effect on the calculated cross sections of interest in all but one case, which will be discussed below. Finally, we ensured that the size of the matrix element for the $2_2^+ \rightarrow 0_1^+$ transition would not affect the resulting $B(E2; 4_1^+ \rightarrow 2_1^+)$.

TABLE I. $B(E2)$ values used in relative Coulomb excitation calculations for ^{98}Ru.

J_i^π	J_f^π	$B(E2)$ W.u.	Reference
2_1^+	0_1^+	29(2)	[5]
2_2^+	2_1^+	55(9)	[5]
2_2^+	0_1^+	1(4)	[5]
2_2^+	0_2^+	0, 1	–

As virtual excitation to higher levels is negligible at our chosen beam energy, the ratio of the 745 keV $4_1^+ \rightarrow 2_1^+$ and 762 keV $2_2^+ \rightarrow 2_1^+$ intensities is equivalent to the ratio of the corresponding excitation cross sections for the 4_1^+ and 2_2^+ levels. In other words,

$$\frac{\sigma(4_1^+)}{\sigma(2_2^+)} = \frac{\sum_f I(4_1^+ \rightarrow J_f^\pi)}{\sum_{f'} I(2_2^+ \rightarrow J_{f'}^\pi)} = c_{\mathrm{BR}} \frac{I_\gamma(4_1^+ \rightarrow 2_1^+)}{I_\gamma(2_2^+ \rightarrow 2_1^+)}, \qquad (1)$$

where $\sum_f I(J_i^\pi \rightarrow J_f^\pi)$ corresponds to the total decay intensity of the initial levels, including unobserved but known radiation, and c_{BR} is a factor obtained from known decay branching ratios. For the 1414 keV 2_2^+ level, the branching ratio $[I_\gamma(2_2^+ \rightarrow 2_1^+) + I_\gamma(2_2^+ \rightarrow 0_1^+)]/I_\gamma(2_2^+ \rightarrow 2_1^+) = 1.50 \pm 0.03$ [9] was used. Since $\sigma(4_1^+)/\sigma(2_2^+)$ varies approximately linearly with respect to the matrix element used for the $4_1^+ \rightarrow 2_1^+$ transition, we were able to extract $B(E2;4_1^+ \rightarrow 2_1^+)/B(E2;2_2^+ \rightarrow 2_1^+)$ (and therefore, the $B(E2;4_1^+ \rightarrow 2_1^+)$ value, assuming $B(E2;2_2^+ \rightarrow 2_1^+) = 55$ W.u.) by comparing $I(4_1^+ \rightarrow 2_1^+)/I(2_2^+ \rightarrow 2_1^+)$ to a linear fit of $\sigma(4_1^+)/\sigma(2_2^+)$ as a function of the $4_1^+ \rightarrow 2_1^+$ matrix element.

The process for extracting the $B(E2;0_2^+ \rightarrow 2_1^+)$ value was virtually identical to that used to determine the $B(E2;4_1^+ \rightarrow 2_1^+)$ value. Since the yield of the 0_2^+ state depends on the $B(E2;4_1^+ \rightarrow 2_1^+)$ value (but not vice versa), we used the $B(E2;4_1^+ \rightarrow 2_1^+)$ value we extracted in determining the $B(E2;0_2^+ \rightarrow 2_1^+)$ value. See Table II for the observed $\sigma(J_i^\pi)/\sigma(2_2^+)$ used to determine both $B(E2)$ values.

TABLE II. $R_{4/2}$, $\sigma(J^\pi)/\sigma(2_2^+)$, $B(E2)$, and $B_{4/2}$ values observed for both ^{98}Ru and ^{180}Pt.

Nucleus	J_i^π	J_f^π	$R_{4/2}$	$\sigma(J_i^\pi)/\sigma(2_2^+)$	$B(E2)$ W.u.	$B_{4/2}$
^{98}Ru	4_1^+	2_1^+	2.14	1.3(4)[a]	50(18)[b,c,d]	1.7(6)[b,c,d]
					59(21)[c,e], 57(21)[d,e]	2.0(7)[c,d,e]
	0_2^+	2_1^+		0.2(1)[a]	36(18)[b,c], 42(21)[b,d]	
					52(26)[c,e], 49(25)[d,e]	
^{180}Pt	4_1^+	2_1^+	2.68		260(32)	1.7(3)

[a]Matrix elements for the $4_1^+ \rightarrow 2_1^+$ and $0_2^+ \rightarrow 2_1^+$ transitions were chosen such that the calculated cross section ratios matched observed cross section ratios. Observed cross section ratios were extracted from Coulomb excitation yields using Eq. 1.

[b]Results determined using the same relative sign for the interfering matrix elements for the excitation of the 2_2^+ state.

[c]Results determined using $B(E2;2_2^+ \rightarrow 0_2^+) = 1$ W.u.

[d]Results determined using $B(E2;2_2^+ \rightarrow 0_2^+) = 0$ W.u.

[e]Results determined using the opposite relative sign for the interfering matrix elements for the excitation of the 2_2^+ state.

Note that there are two routes of deexcitation from the 2_2^+ level (to either the 2_1^+ or 0_1^+ states). The relative sign of the matrix elements for these two routes is unknown, and could not be determined from our experimental results. To account for this, we did two sets of calculations to obtain $\sigma(4_1^+)/\sigma(2_2^+)$ and $\sigma(0_2^+)/\sigma(2_2^+)$: one with a positive matrix element for the $2_2^+ \rightarrow 0_1^+$ transition, and one with a negative corresponding matrix element.

For all sets of calculations, as noted above, test Coulomb excitation calculations including allowed but unobserved transitions from the 2_2^+ state (for example, to the 4_1^+ state) were done to ensure that nonzero matrix elements for such transitions had a negligible effect on our results. We also checked forbidden transitions, to ensure that a small but nonzero $B(E2)$ value in such cases would not have a significant effect on our results. The only case in which we could not ignore such a transition was that of the $B(E2;2_2^+ \rightarrow 0_2^+)$ value. As no absolute $B(E2;2_2^+ \rightarrow 0_2^+)$ value is known, we assumed a $B(E2;2_2^+ \rightarrow 0_2^+)$ value of 1 W.u. in our calculations, because we expect this forbidden transition to be comparable in strength to the known forbidden transition between the 2_2^+ and 0_1^+ states. However, values up to a few W.u. do not significantly effect the results below.

The effect of including the $B(E2;2_2^+ \rightarrow 0_2^+)$ value of 1 W.u. in our calculations on the $\sigma(4_1^+)/\sigma(2_2^+)$ and $\sigma(0_2^+)/\sigma(2_2^+)$ ratios is dependent on the relative sign of the matrix elements for the $2_2^+ \rightarrow 2_1^+$ and $2_2^+ \rightarrow 0_1^+$ transitions. For the case in which the relative sign of these two matrix elements is opposite, $\sigma(4_1^+)/\sigma(2_2^+)$ decreases by 3% and $\sigma(0_2^+)/\sigma(2_2^+)$ decreases by 7% compared to calculations assuming $B(E2;2_2^+ \rightarrow 0_2^+) = 0$ W.u. For the case in which the relative sign of these two matrix elements is the same, $\sigma(4_1^+)/\sigma(2_2^+)$ decreases by less than 1%, and $\sigma(0_2^+)/\sigma(2_2^+)$ increases by 13%. Including even a small matrix element for the $2_2^+ \rightarrow 0_2^+$ transition provides a third means of exciting the 2_2^+ state. For the case in which the relative sign of the two matrix elements is the same, calculations show that this leads to a simultaneous increase in $\sigma(2_2^+)$ and decrease in $\sigma(0_2^+)$, thus resulting in a somewhat larger effect on $\sigma(0_2^+)/\sigma(2_2^+)$.

Results assuming $B(E2;2_2^+ \rightarrow 0_2^+)$ values of 0 W.u. and 1 W.u. are noted in Table II. Assuming $B(E2;2_2^+ \rightarrow 0_2^+) = 1$ W.u., the observed intensity ratios yield $B(E2;4_1^+ \rightarrow 2_1^+) = 59 \pm 21$ W.u. and $B(E2;0_2^+ \rightarrow 2_1^+) = 52 \pm 26$ W.u. for the case in which the relative sign of the interfering matrix elements for the 2_2^+ is opposite. For the case in which the relative signs are the same, $B(E2;4_1^+ \rightarrow 2_1^+) = 50 \pm 18$ W.u. and $B(E2;0_2^+ \rightarrow 2_1^+) = 36 \pm 18$ W.u. This gives a $B_{4/2}$ value of 2.0 ± 0.7 in the case with opposing signs, and 1.7 ± 0.6 in the case with equal signs. Using $B(E2;2_2^+ \rightarrow 0_2^+) = 0$ W.u., the $B_{4/2}$ values for either case are essentially unchanged. In all cases examined here, the resulting $B_{4/2}$ values clearly remove ^{98}Ru from the list of possible anomalies discussed in Ref. [4]; even calculations with $B(E2;2_2^+ \rightarrow 0_2^+) = 5$ W.u. do not yield a $B_{4/2}$ value below 1 within error for either case.

B. ^{180}Pt

The ^{180}Pt nucleus was studied with the RDM technique using the Yale New Yale Plunger Device (N.Y.P.D.) [16].

^{180}Pt was produced using a ^{62}Ni beam of 265 MeV, delivered by the ESTU tandem accelerator. The beam impinged upon a 1 mg/cm^2-thick ^{122}Sn target. The average beam intensity was 0.27 pnA due to the low abundance of the ^{62}Ni isotope. The cross section for the desired ^{122}Sn(^{62}Ni, $4n$)^{180}Pt exit channel was estimated using PACE calculations [12] to be about 100 mb, out of ~300 mb total cross section. The average recoil velocity was $v/c = 0.029(2)$. The gamma radiation was detected by the SPEEDY [13] array, configured as eight Eurisys clover detectors, arranged in two rings about the plunger, each of four detectors, placed at backward ($\theta = 138.5^\circ$) and forward ($\theta = 41.5^\circ$) angles with respect to the beam axis. All detectors were surrounded by BGO Compton suppression shields. The distance between the target and the front end of the detectors was 200 mm; thus, the opening angle was $\pm 13^\circ$ around its center. The master trigger was generated whenever one or more γ rays were detected. The average trigger rate was approximately 400 events per second. The target and stopper foil were stretched and placed parallel to each other in the N.Y.P.D. target chamber, which follows the design of the most recent Cologne plunger [14,15]. The stopper was made out of gold and was 10 mg/cm^2 thick. The target-to-stopper distance was varied during the experiment by using a piezoelectric motor. Target-to-stopper distance was measured using the capacitance method [17]. Data were collected for seven distances between 150 and 600 μm for times ranging between 6 to 12 hs each, with the longer runs assigned to shorter distances. For this experiment, beam was on target for ~4.5 d.

To determine the lifetime of the 4_1^+ level, gates were placed on the shifted component of the $6_1^+ \rightarrow 4_1^+$ transition, and the shifted and unshifted intensities of the 257 keV $4_1^+ \rightarrow 2_1^+$ transition were determined. Figure 4 shows part of a forward angle spectrum in coincidence with the shifted part of the 347 keV $6_1^+ \rightarrow 4_1^+$ transition at back angles. The different panels correspond to spectra collected for three target-to-stopper distances, in which the change in the relative intensities of the Doppler-shifted and unshifted portions of the $4_1^+ \rightarrow 2_1^+$ transition with respect to the change in target-to-stopper distance is visible.

The differential decay curve method (DDCM) [18,19] was used to extract the lifetime from this data. To use this method, one must first ensure that the production of ^{180}Pt is normalized for all distances. The peak intensities were therefore normalized by setting gates on the shifted and unshifted peaks of the $4_1^+ \rightarrow 2_1^+$ and $2_1^+ \rightarrow 0_1^+$ transitions, and choosing a normalization coefficient such that the sum of the shifted and unshifted components for visible higher-lying states remained constant for all distances. The lifetime was then obtained as a ratio:

$$\tau(x) = \frac{I_u(x)}{v\frac{dI_s(x)}{dx}}, \qquad (2)$$

where v is the recoil velocity, x is the target-to-stopper distance, and $I_u(x)(I_s(x))$ is the unshifted(shifted) intensity of the depopulating transition [18]. The lifetime as a function of distance is presented in Fig. 5, along with $I_u(x)$ and $\frac{dI_s(x)}{dx}$. The weighted value of the lifetime obtained from the data is

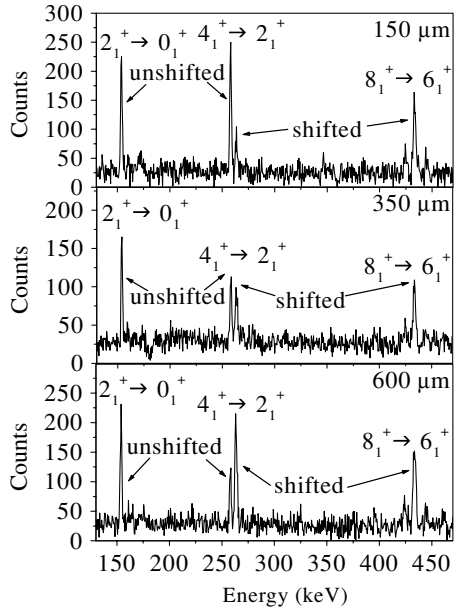

FIG. 4. The ^{180}Pt spectra above result from gating on the $6_1^+ \rightarrow 4_1^+$ transition in the detectors situated at backward angles, and therefore display the coincident radiation at forward angles. The three panels show the same gate at three target-to-stopper distances, to illustrate the ratio of unshifted-shifted intensities for the $4_1^+ \rightarrow 2_1^+$ transition.

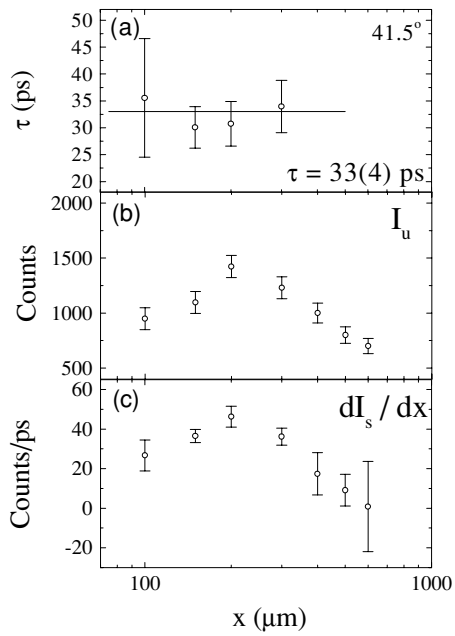

FIG. 5. (a) The resulting lifetime values for the 4_1^+ level in ^{180}Pt as a function of the target-to-stopper distance x. The line corresponds to the weighted average of the lifetime values, which is 33 ± 4 ps. (b) The intensity of the unshifted $4_1^+ \rightarrow 2_1^+$ transition as a function of the target-to-stopper distance, x. (c) The derivative of the intensity of the shifted $4_1^+ \rightarrow 2_1^+$ peak as a function of the target-to-stopper distance, x.

33 ± 4 ps. This value differs greatly from the previously reported value of 75 ± 15 ps [7]. This translates into a $B(E2;4_1^+ \rightarrow 2_1^+)$ value of 260 ± 32 W.u., in contrast to the previous value of 140 ± 30 W.u. The reported $B(E2;2_1^+ \rightarrow 0_1^+)$ of the previous experiment was 153 ± 15 W.u. Assuming this $B(E2;2_1^+ \rightarrow 0_1^+)$ value is correct, the new value for the $B_{4/2}$ ratio is 1.7 ± 0.3, which also removes ^{180}Pt from the list of possible anomalies identified in Ref. [4] for now. The $B(E2;2_1^+ \rightarrow 0_1^+)$ value used to calculate $B_{4/2}$ was obtained in the same experiment that yielded the previous $B(E2;4_1^+ \rightarrow 2_1^+)$ value, however, and should therefore be re-measured for a better determination of the $B_{4/2}$ value for this nucleus.

III. DISCUSSION

A summary of the $B(E2)$ values and $B_{4/2}$ ratios determined for both ^{98}Ru and ^{180}Pt is presented in Table II. Both nuclei exhibit $B_{4/2}$ ratios well above those observed in previous measurements.

In the case of ^{98}Ru, the new measurement conforms to the collective picture. To illustrate this, interacting boson approximation (IBA) model calculations were performed using the extended consistent Q formalism [20] with the Hamiltonian [21,22]

$$H(\zeta) = c\left[(1-\zeta)\hat{n}_d - \frac{\zeta}{4N_B}\hat{Q}^\chi \cdot \hat{Q}^\chi\right], \tag{3}$$

where

$$\hat{Q}^\chi = (s^\dagger \tilde{d} + d^\dagger s) + \chi(d^\dagger \tilde{d})^{(2)}, \tag{4}$$

$$\hat{n}_d = d^\dagger \cdot \tilde{d}, \tag{5}$$

and N_B is the boson number. Calculations were done for $N_B = 5$ because this corresponds to the number of valence bosons in ^{98}Ru if one does not take into account the $Z = 40$ subshell closure (otherwise, $N_B = 4$). The difference in $B_{4/2}$ values for $N_B = 4$ and 5 is small. A contour plot of $B_{4/2}$ for the complete physical range of ζ ($0 \leqslant \zeta \leqslant 1$) and χ ($-1.32 \leqslant \chi \leqslant 0$) made with these calculations can be found in Fig. 6. The U(5), O(6), and SU(3) limits correspond to ($\zeta = 0$, χ unrestricted), ($\zeta = 1$, $\chi = 0$), and ($\zeta = 1$, $\chi = -1.32$), respectively. The low-lying levels of ^{98}Ru exhibit a vibrational structure

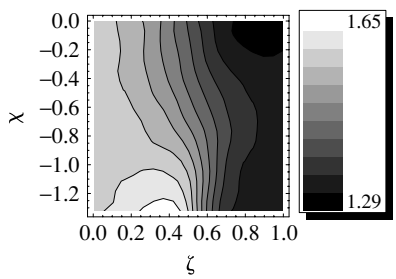

FIG. 6. Contour plot of $B_{4/2}$ values over the entire IBA-1 parameter space for 5 bosons. U(5), located at $\zeta = 0$ for all χ values, corresponds to $B_{4/2} = 1.6$.

($R_{4/2} \equiv E(4_1^+)/E(2_1^+)$, for example, is 2.14), suggesting that the $B_{4/2}$ ratio should be near the $\zeta = 0$ U(5) limit [23]. For $N_B = 5$, in U(5), $B_{4/2} = 1.6$, as shown in Fig. 6. For $N_B = 4$, $B_{4/2} = 1.5$ in U(5). These values agree with our observed $B_{4/2}$ values for both positive and negative relative matrix elements within error, and thus, the $B_{4/2}$ ratio for ^{98}Ru does indeed conform with expectations based on the status of the low-lying levels. As for ^{180}Pt, the new $B_{4/2}$ ratio conforms with the systematic trend reported in the neighboring platinum isotopes within error, as shown in Fig. 1.

IV. CONCLUSION

These experiments remove two of the anomalous nuclei [4] from consideration, but do not finalize this line of inquiry. For one of the other anomalous nuclei, ^{114}Te, recent lifetime measurements [24] have in fact confirmed the anomaly ($B_{4/2} = 0.84(1)$). The remaining seven nuclei, ^{114}Xe, ^{114}Te, ^{132}Nd, ^{134}Ce, ^{134}Xe, ^{144}Nd, and ^{152}Dy, seem to have little in common upon first glance. However, there may be two separate phenomena at work here. Three of the nuclei (^{114}Te, ^{134}Xe, and ^{144}Nd) are only two valence nucleons from the closed shell. Although these nuclei have $B(E2;2_1^+ \rightarrow 0_1^+)$ values >15 W.u., suggesting collective behavior, their $B_{4/2}$ ratios may nevertheless be influenced by single particle effects. In the case of ^{134}Xe, for example, g factor measurements for the 2_1^+ and 4_1^+ states ($g(2_1^+) = +0.354(7)$, $g(4_1^+) = +0.83(14)$) suggest an increase in the proton content for the 4_1^+ state compared to the 2_1^+ state [25]. This is a signature of proton excitation, or dominant single particle degrees of freedom, thus providing a possible explanation for any deviations from known collective models. The ^{134}Xe result may suggest a promising method for understanding the behavior of these three nuclei.

For ^{152}Dy, lingering single particle effects from the $Z = 64$ subshell closure may play some role, but the remaining three nuclei, ^{114}Xe, ^{132}Nd, and ^{134}Ce, do not offer any simple clues as to the reason for their anomalous behavior. These nuclei are unlikely to show any significant single particle effects, considering their distance from any closed shell. As a result, further measurements should be performed to ensure that the reported $B_{4/2}$ values are correct; only then can a full evaluation of the status of this anomalous behavior be made.

ACKNOWLEDGMENTS

The authors would like to thank the staff of the ESTU accelerator at WNSL for their assistance during both experiments, Charles Barton and David Radford for their help with the Coulomb excitation calculations in inverse kinematics, and Noemie Benczer-Koller for help with the angular correlations calculations. This work was supported by U.S. DOE research Grant Nos. DE-FG02-91ER-40609, DE-FG03-03NA-00081, DE-FG-02-88ER-40417, and W-7405-ENG-48 (LLNL), and by the Yale University Flint Fund.

[1] G. Gneuss and W. Greiner, Nucl. Phys. **A171**, 449 (1971).
[2] A. S. Davydov and G. F. Filippov, Nucl. Phys. **8**, 237 (1958).
[3] J. J. Ressler *et al*., Phys. Rev. C **69**, 034317 (2004).
[4] R. B. Cakirli, R. F. Casten, J. Jolie, and N. Warr, Phys. Rev. C **70**, 047302 (2004).
[5] S. Landsberger, R. Lecomte, P. Paradis, and S. Monaro, Phys. Rev. C **21**, 588 (1980).
[6] B. Kharraja *et al*., Phys. Rev. C **61**, 024301 (2000).
[7] M. J. A. De Voigt *et al*., Nucl. Phys. **A507**, 472 (1990).
[8] C. W. Beausang *et al*., Nucl. Instrum. Methods Phys. Res. A **452**, 431 (2000).
[9] B. Singh and Z. Hu, Nucl. Data Sheets **98**, 335 (2003).
[10] A. Winther and J. De Boer, California Institute of Technology, Technical Report, 18 November, 1965; in *Perspectives in Physics Series: Coulomb Excitation*, edited by K. Alder and A. Winther (Academic Press, New York, 1966).
[11] J. F. Ziegler, J. P. Biersack, and U. Littmark, *The Stopping and Range of Ions in Solids* (Pergamon Press, New York, 1985).
[12] A. Gavron, Phys. Rev. C **21**, 230 (1980).
[13] R. Krücken, *Proceedings of the International Conference on Applications of Accelerators in Research and Industry*, CAARI, 2000 (AIP, New York, 2001), p. 319.
[14] A. Dewald, Cologne plunger, University of Cologne (unpublished).
[15] A. Dewald *et al*., Nucl. Phys. **A545**, 822 (1992).
[16] R. Krücken, J. Res. Natl. Inst. Stand. Technol. **105**, 53 (2000).
[17] T. K. Alexander and A. Bell, Nucl. Instrum. Methods **81**, 22 (1970).
[18] A. Dewald, S. Harissopulos, and P. von Brentano, Z. Phys. A **334**, 163 (1989).
[19] G. Böhm, A. Dewald, P. Petkov, and P. von Brentano, Nucl. Instrum. Methods Phys. Res. A **329**, 248 (1993).
[20] P. O. Lipas, P. Toivonen, and D. D. Warner, Phys. Lett. **B155**, 295 (1985).
[21] N. V. Zamfir, P. von Brentano, R. F. Casten, and J. Jolie, Phys. Rev. C **66**, 021304(R) (2002).
[22] V. Werner, N. Pietralla, P. von Brentano, R. F. Casten, and R. V. Jolos, Phys. Rev. C **61**, 021301(R) (2000).
[23] F. Iachello and A. Arima, *The Interacting boson model* (Cambridge University Press, Cambridge, 1987).
[24] O. Möller, N. Warr, J. Jolie, A. Dewald, A. Fitzler, A. Linnemann, K. O. Zell, P. E. Garrett, and S. W. Yates, Phys. Rev. C **71**, 064324 (2005).
[25] G. Jakob *et al*., Phys. Rev. C **65**, 024316 (2002).